

# Systematic staging design applied to the fixed-bed reactor series for methanol and one-step methanol/dimethyl ether synthesis

Flavio Manenti<sup>a,\*</sup>, Andres R. Leon-Garzon<sup>a</sup>, Zohreh Ravaghi-Ardebili<sup>a</sup>, Carlo Pirola<sup>b</sup>

<sup>a</sup>Politecnico di Milano, Dipartimento di Chimica, Materiali e Ingegneria Chimica "Giulio Natta", Piazza Leonardo da Vinci 32, Milano 20133, Italy

<sup>b</sup>Università degli Studi di Milano, Dipartimento di Chimica, Via Golgi 19, Milano 20133, Italy

Received 4 January 2014

Received in revised form

2 April 2014

Accepted 4 April 2014

Available online 15 April 2014

## 1. Introduction

Since the introduction of the high pressure methanol synthesis in the 1920s, several technologies have been introduced or are currently in development [2]; however the most important improvement is the introduction of the low pressure methanol synthesis in the 1960s, in fact several of the current technologies, like those available from Lurgi [3], Haldor Topsøe [4] and Davy Process Technologies [5], are based in such development. Nowadays, methanol is still produced from syngas (CO and H<sub>2</sub> mixture) obtained by means of steam reforming operations of natural gas [6], most of the aforementioned technologies employ a single water-cooled shell and tube boiler reactor (WaC) and therefore a great attention has been given to the study of such reactor by researchers.

For instance, Shahrokhi and Baghmisheh [7] investigated the dynamic behavior and proposed a control strategy of the WaC portion of the reactor. Chen and co-workers [8] studied the WaC reactor and the related boiling system to optimize the yield in methanol synthesis. They obtained a methanol yield improvement estimated in about 7%. Similarly, our prior works investigated the steady-state optimal configuration of the WaC reactor [9], its dynamic behavior subject to possible syngas composition and inlet flow variations [10], the simultaneous control of the methanol production and hot-spot temperature position along the axial coordinate [11] and the monitoring strategy of the hot spot for methanol yield improvement [12]. On the other hand, another usual technology for the production of methanol consist of a couple of reactors: (1) a gas-cooled shell and tube reactor (GaC) and (2) the solely WaC reactor; the implementation of the GaC reactor implies a series of technical advantages in process intensification that will be discussed later. The WaC reactor is considered the key section of the overall system and, as indicated earlier, there is plenty of works on

\* Corresponding author. Tel.: +39 02 2399 3273; fax: +39 02 7063 8173.  
E-mail address: flavio.manenti@polimi.it (F. Manenti).

such reactor but the GaC portion is usually rejected. A typical WaC/GaC length ratio of 7/3 is normally used in industry; such ratio is near to the optimal design of the WaC reactor since the target is the optimization of methanol yield. Nonetheless, there are two aspects that should be accounted to improve the total revenue that does not generally imply any additional costs which are: (1) the optimization of the overall WaC/GaC reactor series; rather than optimizing only the sole WaC reactor, it is possible to exploit the integrated model of the WaC/GaC series to perform an overall design optimization to maximize the methanol yield; (2) the integration of energy production as medium pressure steam within the optimization procedure [13] according to the general energy policies also adopted in other closest fields [14]. The main objective of the current work is focused in the previous two elements; therefore, following the systematic staging design methodology by Hillestad [1] comprising the whole reactor system (i.e. both the WaC and GaC reactor) and considering the economic terms involved in both production yield and energy-process integration, a review of the optimal reactor configuration is presented for the production of methanol and also for the simultaneous production of methanol and dimethyl ether. Consequently, in Section 2 the methanol synthesis and the dimethyl ether processes are described followed by a description of the pseudo-homogeneous model in Section 3. In Section 4 the systematic staging design strategy is reviewed and finally in Section 5 the optimization strategy is described together with the numeric results and economic considerations.

## 2. Methanol and dimethyl ether synthesis process

As mentioned above, the methanol synthesis process is usually based on two fixed-bed tubular reactors [15], although several other configurations have been proposed [16]. According to the final production target, methanol synthesis can be coupled with the dimethyl ether synthesis which is usually obtained in a two-step process; in this, the first reactor system is employed for the synthesis of methanol which is followed by a second reactor system for the production of dimethyl ether from methanol. Coupling both systems in a one-step process allows to employ a single reactor system with a bifunctional catalyst for the simultaneous production of both methanol and dimethyl ether in a process called direct dimethyl ether synthesis; this is of key-relevance especially when the syngas originates from renewable sources (e.g., biomass) as discussed elsewhere [17]. Following the process flow direction of Fig. 1, the syngas is fed to the shell side of the gas-cooled reactor (Stream 1), where it is pre-heated by the hot process stream flowing in the fixed-bed tube bundle, this is advantageous in terms of process intensification as the usually large inlet pre-heater is

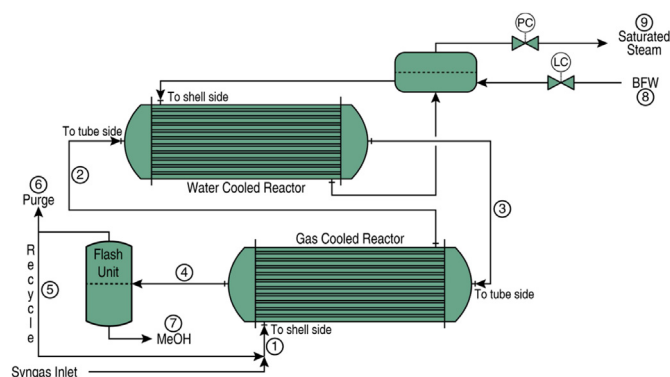
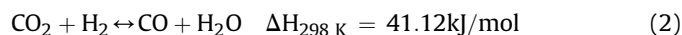
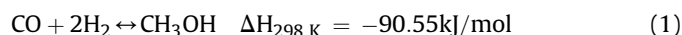


Fig. 1. Methanol synthesis loop with water/gas-cooled (WaC/GaC) reactors.

replaced by a smaller unit and reducing in the same way the consumption of process utilities. The pre-heated syngas is then fed to the catalytic bed for methanol conversion and specifically to the tube side of the WaC reactor (Stream 2). Please note that different technologies may have the catalyst in the shell side (e.g., Davy Process technology), but they are not considered for the sake of simplicity and conciseness. The syngas fed to the fixed-bed of the catalytic tube bundle is partially converted into methanol along the first reactor. The methanol synthesis is particularly exothermic and the shell side is filled of boiling water (Stream 8) to preserve the desired operating conditions of the WaC reactor. The intrinsic intensified nature of modern methanol process allows to combine the methanol conversion to the medium pressure steam generation (Stream 9). As discussed in previous works [9], the phenomena occurring in the first portion of the reactor (first 1–2 m along the reactor) is kinetically limited, while in the later part the chemical equilibrium plays a major role limiting the reaction. In this first part a point with maximum temperature is developed called temperature hot-spot. The importance of the hot-spot is critical in order to improve not only the process efficiency but also to preserve the catalyst activity and process safety [18] and some special techniques are required to monitor it [11]. Continuing with the process flow, the outflow of the WaC reactor is fed to the tube side of the GaC reactor (Stream 3) where the methanol synthesis continues. GaC temperature profile is controlled exchanging with the fresh inlet syngas to be pre-heated in countercurrent in the shell side (Stream 1). The GaC reactor outflow (Stream 4) is then sent to the downstream process where the methanol is recovered (Stream 7) and the unreacted syngas is recycled back (Stream 5) except a purge system to remove by-products, and accumulations of incondensable gas (Stream 6).

### 2.1. Methanol synthesis

Methanol (MeOH) is produced from syngas from three main reactions:



These reactions are not independent and any one of them can be expressed as a linear combination of the others as indicated elsewhere. Rather than using the chemical species, as in the typical mathematical modeling of chemical reactors, the chemical elements C, H, and O must be considered to reduce the size of the resulting numerical system [10]. Exothermic reactions (1) and (3) are favored at low temperature despite the reaction rate; moreover, it is necessary to operate at high pressure (for instance 80 bar) to improve the equilibrium conversion exploiting the reduction in the number of moles. Typically, the synthesis of methanol is conducted over commercial  $\text{CuO}/\text{ZnO}/\text{Al}_2\text{O}_3$  which has an estimated life of 3–4 years. Since catalyst deactivation occurs at temperatures above the 550 K, the operating range of temperature is 484 K–540 K. Typical feed molar composition is:  $\text{CO} = 0.046$ ;  $\text{CO}_2 = 0.094$ ;  $\text{H}_2 = 0.659$ ;  $\text{H}_2\text{O} = 0.0004$ ;  $\text{CH}_3\text{OH} = 0.005$ ;  $\text{N}_2 = 0.093$ ;  $\text{CH}_4 = 0.1026$  [15].

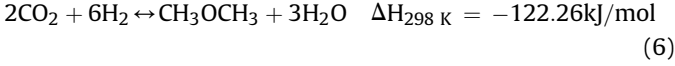
### 2.2. Direct dimethyl ether synthesis

Dimethyl ether (DME) is a promising efficient alternative fuel for diesel engines as it possesses a high cetane number, produces a smoke-free combustion due to its high oxygen content and has a

low boiling point that allows a quick vaporization inside the engine cylinders. It is produced traditionally in a two-step process which involves the synthesis of methanol in a single reactor followed by a second reactor for the dehydration of methanol into DME:



Nonetheless, it is possible to join both processes into a one-step process when combining the methanol dehydration reaction in Eq. (4) with the methanol synthesis reactions in Eqs. (1) and (3):



The resulting process is called direct dimethyl ether synthesis and employs a bifunctional catalyst composed by the already known CuO/ZnO/Al<sub>2</sub>O<sub>3</sub> for methanol synthesis coupled with  $\gamma$ -Al<sub>2</sub>O<sub>3</sub> for the methanol dehydration. Reaction (4) is also limited by the equilibrium but it does not have such a detrimental effect as with the methanol synthesis reaction. As a result, being an exothermic reaction with no change in the number of moles, it is favored at low temperatures but is not affected by a change on the system pressure. Typical feed molar composition is: CO = 0.17; CO<sub>2</sub> = 0.0404; H<sub>2</sub> = 0.4282; H<sub>2</sub>O = 0.0002; CH<sub>3</sub>OH = 0.003; DME = 0.0018; N<sub>2</sub> = 0.3129; CH<sub>4</sub> = 0.0435 [19].

In both methanol and methanol/dimethyl ether synthesis processes the presence of the products in the reactor's feed composition are due to the unavoidable recycle of the unreacted syngas as both processes are characterized by a low yield.

### 3. Mathematical modeling

The mathematical modeling of the overall system can be divided into three main components: (1) the WaC reactor; (2) the GaC reactor and (3) the preliminary phase separation for syngas recycle from the raw methanol. The mathematical model developed for the simulation of the methanol production loop is based on the assumption of negligible axial and radial diffusion, constant radial velocity, constant temperature and pressure profiles within the catalytic pellet, negligible catalyst deactivation and side reactions, and catalytic particle efficiency using modified Thiele modulus:

$$\phi_i = \frac{r_p}{3} \sqrt{\frac{k'_j (k_j^{\text{eq}} + 1)}{D_e^j k_j^{\text{eq}}}} \quad \eta_i = \frac{1}{\phi_i} \frac{(3\phi_i \coth(3\phi_i) - 1)}{3\phi_i} \quad (7)$$

where  $\phi_i$  is the modified Thiele modulus,  $r_p$  is the radius of the catalytic pellet,  $k'_j$  is the pseudo-first-order constant of the  $j$ th reaction,  $k_j^{\text{eq}}$  is the equilibrium constant of the  $j$ th reaction;  $D_e^j$  is the effective diffusivity of the  $j$ th component of the mixture as specified by Lommerts et al [20]. The linearized kinetics required to achieve  $k'_j$  for methanol and water are, respectively:

$$r'_{\text{CH}_3\text{OH}} = k'_{\text{CH}_3\text{OH}} \left( C_{\text{H}_2} - \frac{C_{\text{CH}_3\text{OH}}}{k_{\text{CH}_3\text{OH}}^{\text{eq}}} \right) \quad r'_{\text{H}_2\text{O}} = k'_{\text{H}_2\text{O}} \left( C_{\text{H}_2} - \frac{C_{\text{H}_2\text{O}}}{k_{\text{H}_2\text{O}}^{\text{eq}}} \right) \quad (8)$$

and are obtained by replacing the  $r$ ,  $k_{\text{eq}}$  and concentration values calculated at the integration step. The kinetic laws adopted were already proposed elsewhere [21]:

$$r_1 = \frac{k_1 K_{\text{CO}} \left[ f_{\text{CO}} f_{\text{H}_2}^{1.5} - \frac{f_{\text{CH}_3\text{OH}}}{f_{\text{H}_2}^{0.5} K_{p1}} \right]}{(1 + K_{\text{CO}} f_{\text{CO}} + K_{\text{CO}_2} f_{\text{CO}_2}) \left[ f_{\text{H}_2}^{0.5} + \left( \frac{K_{\text{H}_2\text{O}}}{K_{\text{H}_2}^{0.5}} \right) f_{\text{H}_2\text{O}} \right]} \quad (9)$$

$$r_2 = \frac{k_2 K_{\text{CO}_2} \left[ f_{\text{CO}_2} f_{\text{H}_2} - \frac{f_{\text{CO}} f_{\text{H}_2\text{O}}}{K_{p2}} \right]}{(1 + K_{\text{CO}} f_{\text{CO}} + K_{\text{CO}_2} f_{\text{CO}_2}) \left[ f_{\text{H}_2}^{0.5} + \left( \frac{K_{\text{H}_2\text{O}}}{K_{\text{H}_2}^{0.5}} \right) f_{\text{H}_2\text{O}} \right]} \quad (10)$$

$$r_3 = \frac{k_3 K_{\text{CO}_2} \left[ f_{\text{CO}_2} f_{\text{H}_2}^{1.5} - \frac{f_{\text{CH}_3\text{OH}} f_{\text{H}_2\text{O}}}{f_{\text{H}_2}^{1.5} K_{p3}} \right]}{(1 + K_{\text{CO}} f_{\text{CO}} + K_{\text{CO}_2} f_{\text{CO}_2}) \left[ f_{\text{H}_2}^{0.5} + \left( \frac{K_{\text{H}_2\text{O}}}{K_{\text{H}_2}^{0.5}} \right) f_{\text{H}_2\text{O}} \right]} \quad (11)$$

The most common way to consider the production of dimethyl ether when employing a bifunctional catalyst is to couple two kinetic models, one for the synthesis of methanol (see above) and another for the methanol dehydration described by Berčić & Levec [22]:

$$r_4 = \frac{k_4 K_{\text{CH}_3\text{OH}}^2 \left( C_{\text{CH}_3\text{OH}}^2 - \frac{C_{\text{H}_2\text{O}} C_{\text{DME}}}{K_{c4}} \right)}{\left( 1 + 2(K_{\text{CH}_3\text{OH}} C_{\text{CH}_3\text{OH}})^{1/2} + K_{\text{H}_2\text{O}} C_{\text{H}_2\text{O}} \right)^4} \quad (12)$$

The GaC and WaC reactors are modeled assuming that concentration and temperature gradients between the gas and solid phase are negligible, significantly simplifying the numerical solution and reducing the computation effort without losing in accuracy [9]. Constitutive equations for the WaC reactor model are:

Mass balance:

$$\frac{M}{A_i} \frac{d\omega_i}{dz} = MW_i \rho_{\text{cat}} (1 - \varepsilon_b) \sum_j^{NR} \nu_{ij} \eta_j r_j \quad (13)$$

WaC and GaC energy balance:

$$\frac{M c_{p_{\text{mix}}}}{A_i} \frac{dT}{dz} = \pi \frac{D_i}{A_i} U_{\text{tube}} (T_{\text{shell}} - T) + \rho_{\text{cat}} (1 - \varepsilon_b) \sum_j^{NR} (-\Delta H_j^{\text{rxn}}) \eta_j r_j \quad (14)$$

Ergun equation:

$$\frac{dP}{dz} = - \left( 1.75 + 150 \left( \frac{1 - \varepsilon_b}{\text{Re}} \right) \right) \frac{u^2 \rho_{\text{gas}}}{d_p} \frac{1 - \varepsilon_b}{\varepsilon_b^3} \quad (15)$$

Equations are the same for GAC reactor, but the additional energy balance to characterize the coolant gas flowing in counter-current is needed:

GaC's shell energy balance:

$$\frac{M c_{p_{\text{mix}}}}{A_i} \frac{dT_{\text{shell}}}{dz} = -\pi \frac{D_i}{A_i} U_{\text{shell}} (T - T_{\text{shell}}) \quad (16)$$

Finally, the preliminary separation for the syngas recycle consists of a simple flash drum separator, the total (17) and component mass balances (18)–(20) are:

$$F = V + L \quad (17)$$

$$F z_{f,i} = V y_i + L x_i \quad (18)$$

**Table 1**  
Reactor and catalyst specifications.

|                      | MeOH synthesis        | MeOH/DME synthesis   |                      |
|----------------------|-----------------------|----------------------|----------------------|
| Total length         | 7                     | 7                    | [m]                  |
| $D_i$                | 0.0341                | 0.046                | [m]                  |
| $D_o$                | 0.0381                | 0.05                 | [m]                  |
| Void fraction        | 0.39                  | 0.39                 | [-]                  |
| Pressure             | 7.698                 | 5                    | [MPa]                |
| Inlet Temperature    | 484.0                 | 446.0                | [K]                  |
| Catalyst density     | 1770                  | 1783.5               | [kg/m <sup>3</sup> ] |
| Catalyst diameter    | $5.47 \times 10^{-3}$ | $5.0 \times 10^{-3}$ | [m]                  |
| $\varepsilon_c/\tau$ | 0.123                 | 0.269                | [-]                  |
| Number of tubes      | 2962                  | 2962                 | [-]                  |

$$\sum_{i=1}^N y_i = 1 \quad (19)$$

$$\sum_{i=1}^N x_i = 1 \quad (20)$$

Given flash separator conditions, the solution is found adopting the method proposed by Rachford and Rice [23]:

$$f(V/F) = \sum_{i=1}^N \frac{z_{f,i}(K_{EoS,i} - 1)}{\frac{V}{F}(K_{EoS,i} - 1) + 1} = 0 \quad (21)$$

Were  $K_i$  are the K-values and were calculated using an appropriate equation of state:

$$K_{EoS,i} = \frac{y_i}{x_i} = \frac{\phi_i^l}{\phi_i^v} \quad (22)$$

The specification of the reactor and the catalyst employed throughout the simulations are listed in Table 1. The kinetics of reaction and the auxiliary correlations employed are included in Appendix A and B respectively.

#### 4. Systematic staging design

The particular configuration of the methanol synthesis reactor allows to review the staged design employing the systematic staging strategy proposed by Hillestad [1]. Such methodology covers essentially a model formulation and an optimization procedure of the so-called ‘reactor path’ defined by the author as the line of production in which a series of operations take place. Several parameters can be employed in order to assess different design

function (see Table 1), nonetheless the most interesting parameters in this particular case are those related to (1) the exchange area distribution which is directly related to the WaC/GaC length ratio; (2) the temperature of the coolant (i.e. temperature of the boiling water in the WaC reactor) due to the highly exothermic nature of the reaction; and (3) the employment of the bifunctional catalyst in order to exploit the synergistic effect of coupling both the synthesis of methanol and dimethyl ether in a single step.

#### 4.1. Sensitivity analysis

A series of sensitivity analysis were made in order to familiarize with the influence on the described model by a modification on the parameters due to the application of the systematic staging strategy. Two cases were considered, one for the synthesis of methanol and another for the coupled synthesis of both methanol and dimethyl ether using the bifunctional catalyst, for both the parameters of interest were the WaC/GaC length ratio and the coolant’s temperature.

##### 4.1.1. Variation of WaC/GaC length ratio in methanol synthesis

It can be seen from Fig. 2(a) that diminishing the value of WaC/GaC length ratio the temperature of the hot spot in the WaC reactor is higher due to a higher inlet temperature as the syngas feed is allowed to heat further in the GaC reactor. Additionally, as long as the WaC/GaC length ratio decreases a second hot spot will be produced in the GaC reactor as the kinetic of the reaction will still be relevant in such reactor. The profiles of methanol mole fraction are shown in Fig. 2(b), as expected, for low values of WaC/GaC length ratio the methanol mole fraction is higher as the kinetic of reaction is improved by the higher temperature, nonetheless, for such values the catalyst might suffer a permanent damage and a proper constraint must be considered for the optimization study.

##### 4.1.2. Variation of coolant temperature in methanol synthesis

Fig. 3(a) shows the effect of the coolant temperature on the temperature along the reactor, as expected, due to the exothermicity of the reaction, high coolant temperatures are detrimental for the catalyst as the hot spot reaches high values of temperature, there is also a sudden drop in the methanol fraction in Fig. 3(b) indicating the unfavorable effect of the thermodynamic equilibrium on the reaction. Similar to the case aforesaid, for low values of coolant temperature, which results in a low temperature profile along the reactor, a second hot spot is developed as the kinetic of the reaction is still important in this later stage.

As seen in Figs. 2 and 3, the reaction path is heavily influenced by the selected parameters; in fact lower values of WaC/GaC length

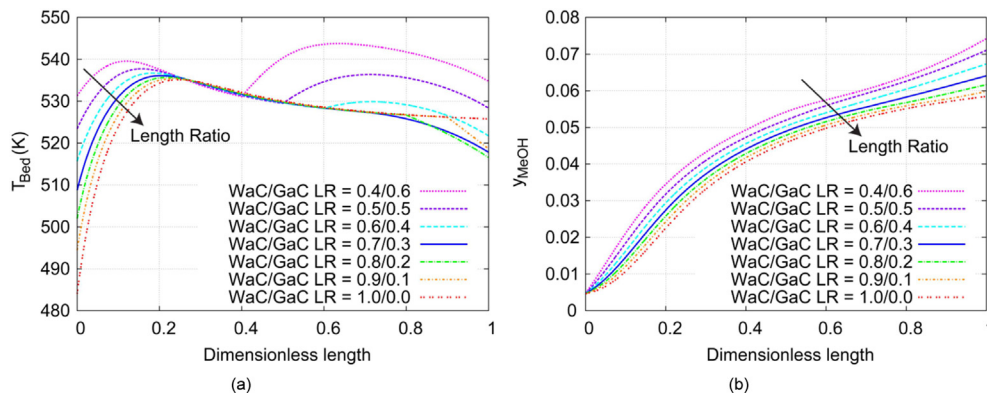


**Fig. 2.** Effect of WaC/GaC length ratio variation on profiles of (a) bed temperature and (b) methanol mole fraction in methanol synthesis process.

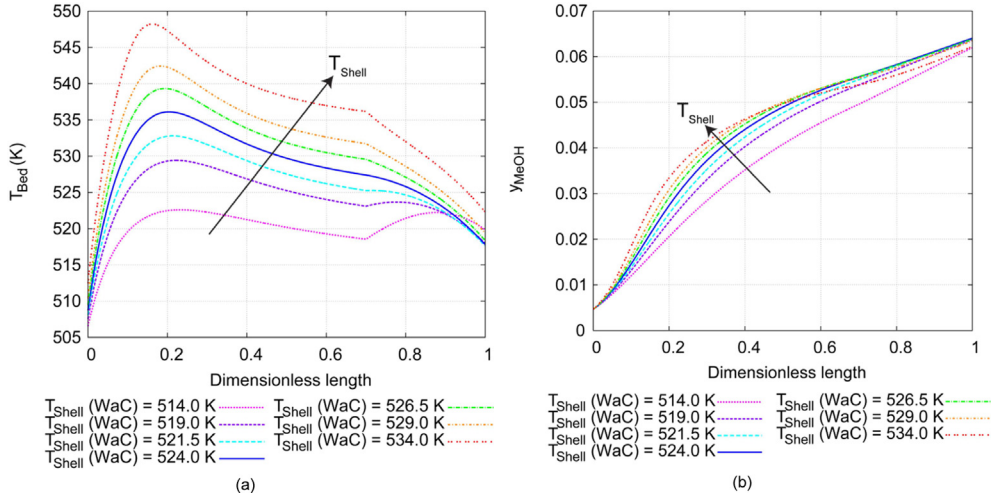


Fig. 3. Effect of coolant temperature variation on profiles of (a) bed temperature and (b) methanol mole fraction in methanol synthesis process.

ratio shifts the temperature profile to the left of the traditional path while decreasing the WaC's shell temperature shifts it below the same. As a result, due to the effect of the parameters on the reaction's kinetics and the bed's temperature discussed above, it is expected that the optimized profile will lie in lower values of temperature and WaC/GaC ratio than the traditional profile, thus increasing the methanol yield while also respecting the hot spot temperature constraint in order to safeguard the catalyst.

#### 4.1.3. Variation of WaC/GaC length ratio in direct dimethyl ether synthesis

The effect of the WaC/GaC length ratio on the direct dimethyl ether synthesis temperature profile is shown in Fig 4(a); similar results were obtained to those of the methanol synthesis process, however the peaks of the hot spot are steeper as a result of the increased exothermicity when coupling both systems of reaction, therefore the control of temperature is critical to avoid damages on the catalyst. The profiles along the reactor of the methanol mole fraction and dimethyl ether mole fraction are shown in Fig. 4(b) and (c), it is possible to observe that the limitations of the thermodynamic equilibrium on the dimethyl ether synthesis are less adverse when comparing with the methanol synthesis reaction as there is no sudden drop in the molar fraction profile; this will result in a synergistic effect relieving the unfavorable thermodynamics of methanol synthesis and therefore a higher syngas conversion.

#### 4.1.4. Variation of coolant temperature in direct dimethyl ether synthesis

As shown in Fig. 5(a), the effect of the coolant temperature is more evident in the temperature profile of the direct dimethyl ether synthesis, once more, a second hot spot is developed in correspondence to low values of coolant temperature. Nonetheless from Fig. 5(c) the effect of this parameter on the final dimethyl ether molar fraction is not significant even though the profile is clearly affected.

The variation of the selected parameters in the methanol/dimethyl ether synthesis process produces a similar behavior in the reaction path to that of the sole methanol synthesis process as seen Figs. 4 and 5. Once more, decreasing the value of the WaC/GaC length shifts the profile to the left of the traditional one, while lowering the WaC's temperature shifts it below. Nonetheless, while a variation in the WaC's temperature affects mostly the methanol yield the modification of the WaC/GaC length ratio influences not

only the methanol but also the dimethyl ether yield. On the other hand, slightly modifying WaC's temperature produces a considerable change in the bed's temperature due to the higher exothermicity of the reaction system. Hence, it is expected that the optimized reaction path will lie in lower values of WaC/GaC length ratio while the WaC's temperature will not be greatly modified.

## 5. Optimization

### 5.1. Methanol synthesis process optimization

Based on the results previously obtained it is possible to optimize the selected degrees of freedom. As already stated, the first interesting parameter is the WaC/GaC length ratio, which is generally assumed equal to 7/3 (2.333) for the industrial best practice in many cases for the methanol synthesis reactor and assumes a value equal to 1 in the conventional dimethyl ether synthesis as there is no gas-cooled reactor [24]. The second interesting parameter is the coolant temperature, that assumes a value of 524 K for the methanol synthesis reactor [25] and a value of 513 K for the conventional dimethyl ether synthesis reactor [24]. According to Manenti et al. [26] a significant review can be made to the overall design if an integrated energy-process optimization is made instead of the common process optimization.

$$\begin{aligned}
 & \max && y_{\text{MeOH}} \\
 & \text{WaC/GaC ratio} \\
 & \text{WaC shell temp} \\
 & \text{s.t : WaC and GaC models(DAE)} \\
 & \text{path constraint : } T < 540 \text{ K}
 \end{aligned} \tag{23}$$

$$\begin{aligned}
 & \max && y_{\text{MeOH}} + F_{\text{Steam}} \\
 & \text{WaC/GaC ratio} \\
 & \text{WaC shell temp} \\
 & \text{s.t : WaC and GaC models(DAE)} \\
 & \text{path constraint : } T < 540 \text{ K}
 \end{aligned} \tag{24}$$

The case illustrated in (23) is typical of a process optimization where only the methanol yield is maximized while the latter case (24) implies the concurrent maximization of methanol yield and steam generation. Comparing the temperature profiles of Fig. 6(a) obtained for the energy process optimization (24) with respect to the traditional process, it seems that the WaC/GaC length ratio dramatically drops to 0.527/0.473 radically changing the system

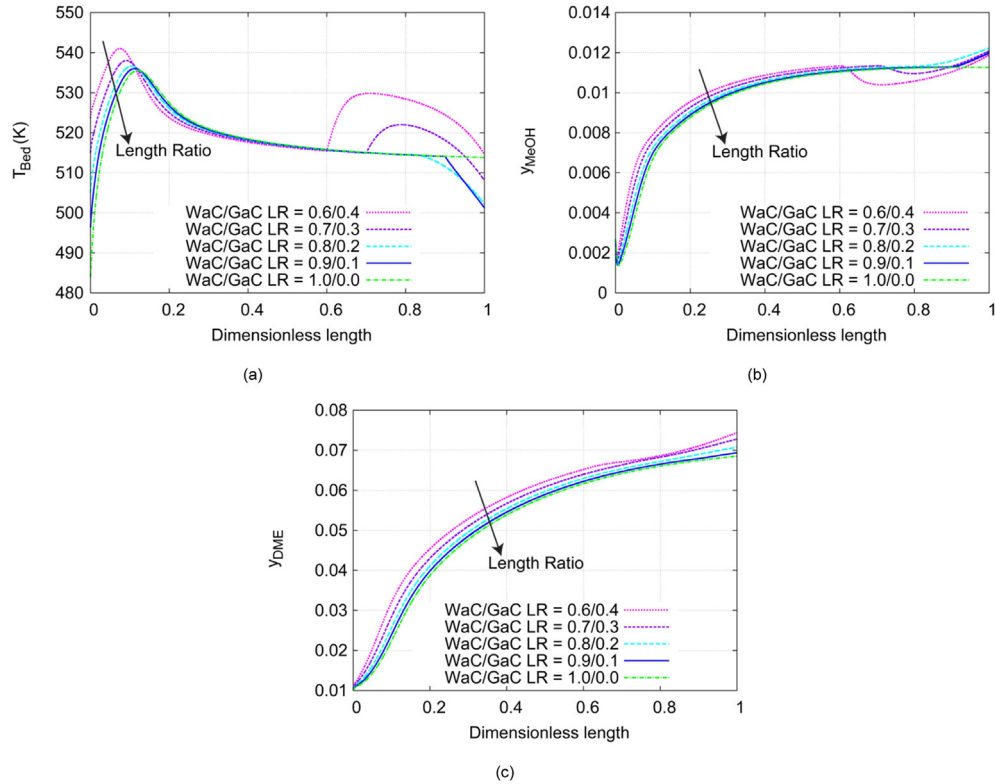


**Fig. 4.** Effect of WaC/GaC length ratio variation on profiles of (a) bed temperature; (b) methanol mole fraction; and (c) dimethyl ether mole fraction in direct dimethyl ether synthesis process.

and increasing the methanol yield, as shown in Fig. 6(b). Therefore, the implementation of a systematic staging provides a flexible and comprehensive design of reactor systems if suitable and sufficient parameters are employed in the optimization, even when the complexity of the design is further increased, the benefits clearly surpasses such limitations and emphasizes the importance of considering the overall reactor system in the optimal design of methanol synthesis process. On the other hand, also from Fig. 6 it is shown that the difference between the process optimization and the energy process optimization is not substantial, as the optimization was made in economical terms it can be explained by the fact that more revenue is obtained from the production of methanol than from steam generation, nonetheless such term was also maximized but in a lesser extent.

As expected, the optimized profile is a combination of a lower WaC/GaC length ratio and WaC's temperature, therefore shifting the bed-s temperature profile to the left and below the traditional one, thus causing the cross between the optimized and non-optimized temperature profiles observed in Fig. 6(a).

Table 2 shows the economic and the resulting process variable comparison of the different configurations reviewed along with the carbon conversion defined in (25), it is independent on the extent of the WGS reaction as it is not disturbed by the production and consumption of CO and CO<sub>2</sub> in such reaction. The economic estimation was done considering the revenue coming from methanol and energy (in form of MP steam) production on a yearly basis, a methanol price equal to €370 per ton<sup>1</sup> [27] and an indicative energy price of €0.1/kJ<sup>2</sup> were employed. As a result, there is an

additional revenue of 3.68% for the process optimization and of 3.79% for the energy process optimization.

$$\text{Carbon Conversion} = \frac{(F_{\text{CO}} + F_{\text{CO}_2})_{\text{inlet}} - (F_{\text{CO}} + F_{\text{CO}_2})_{\text{outlet}}}{(F_{\text{CO}} + F_{\text{CO}_2})_{\text{inlet}}} \quad (25)$$

## 5.2. Dimethyl ether synthesis process optimization

Following the same path of the methanol synthesis process it is possible to optimize the dimethyl ether synthesis process while employing and energy process optimization as shown in (26). Fig. 7(a) and (b) shows that the implementation of the GaC stage allows a subtle increase in the methanol yield but almost no variation in the dimethyl ether synthesis, this is explained once again by the severe effect of the equilibrium in methanol synthesis which is alleviated by the lower temperatures of the GaC stage, however as such effect is not significant in the dimethyl ether synthesis no advantages are obtained from the implementation of the GaC stage on its profile. Once again, the economic estimation was done considering the revenue from methanol/dimethyl ether and energy (from MP steam) production in a yearly basis, an indicative dimethyl ether price equals to €665 per ton was employed [28]. Only an additional revenue of 0.9% is obtained for the energy process optimization, nonetheless, recalling that the implementation of a different catalyst is also part of the staging strategy, the greatest improvement comes from the carbon conversion which is increased from about 30% in the methanol synthesis process (see Table 3) to around 50% (see Table 4) in the methanol/dimethyl ether synthesis process.

<sup>1</sup> Indicative european price for the January 1 to March 31, 2013 period.

<sup>2</sup> Internal communication.

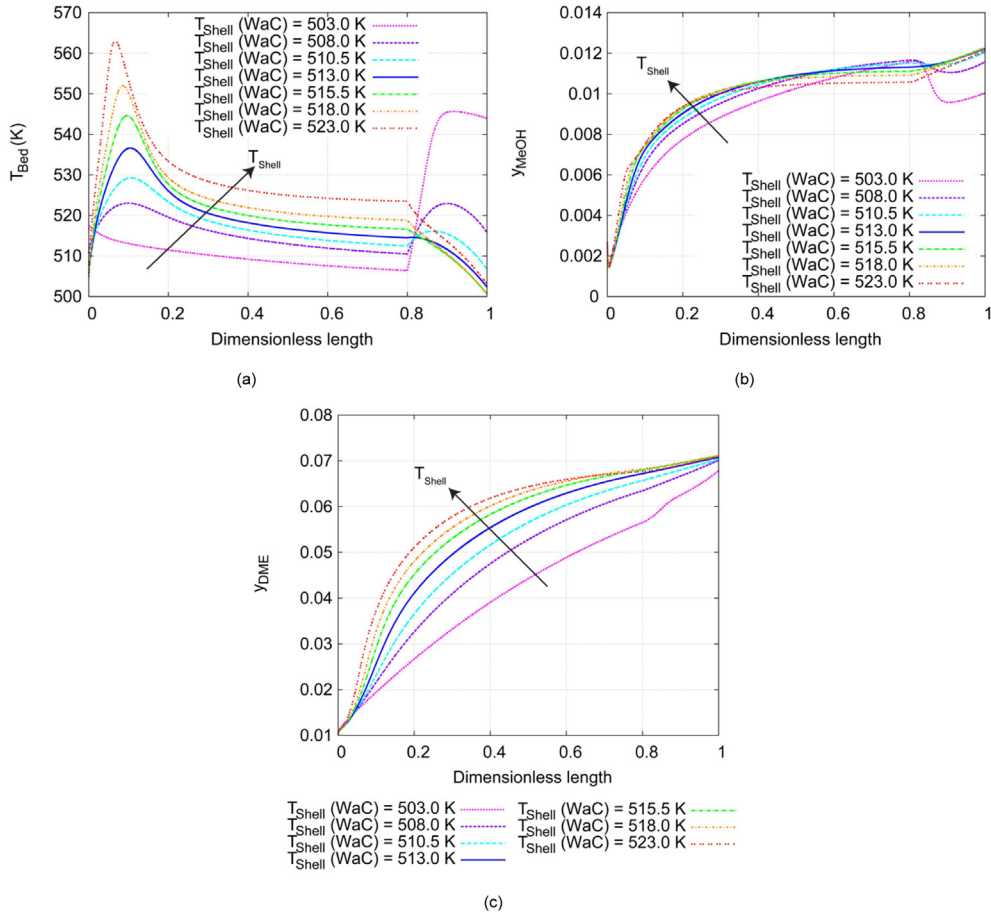


**Fig. 5.** Effect of coolant temperature variation on profiles of (a) bed temperature; (b) methanol mole fraction; and (c) dimethyl ether mole fraction in direct dimethyl ether synthesis process.

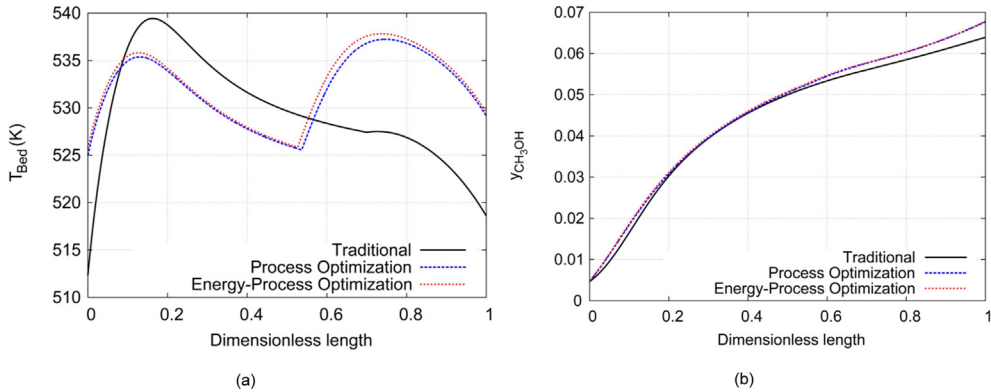


**Fig. 6.** Profile comparison between the traditional; the process optimization; and the energy process optimization for (a) temperature and (b) methanol mole fraction in methanol synthesis process.

**Table 2**  
Mapping of basic operations and design functions (Hillestad, 2010).

| Basic operation   | Design function                                      |
|-------------------|--|
| Fluid mixing      | Mixing   |
| Chemical reaction | Catalyst dilution<br>Different catalyst types        |
| Heat exchange     | Exchange area distribution<br>Temperature of coolant |
| Extra feeding     | Feed distribution<br>Feed composition/temperature    |
| Pressure change   | Pressure profile                                     |

$$\begin{aligned}
 & \max && Y_{\text{MeOH}} + Y_{\text{DME}} + F_{\text{Steam}} \\
 & \text{WaC/GaC ratio} \\
 & \text{WaC shell temp} \\
 & \text{s.t : WaC and GaC model(DAE)} \\
 & \text{path constraint : } T < 540 \text{ K}
 \end{aligned} \tag{26}$$

## 6. Conclusions

This work presented the possibility of a revision of the methanol synthesis process following the systematic staging strategy defined by Hillestad [1] in order to increase the methanol yield while also

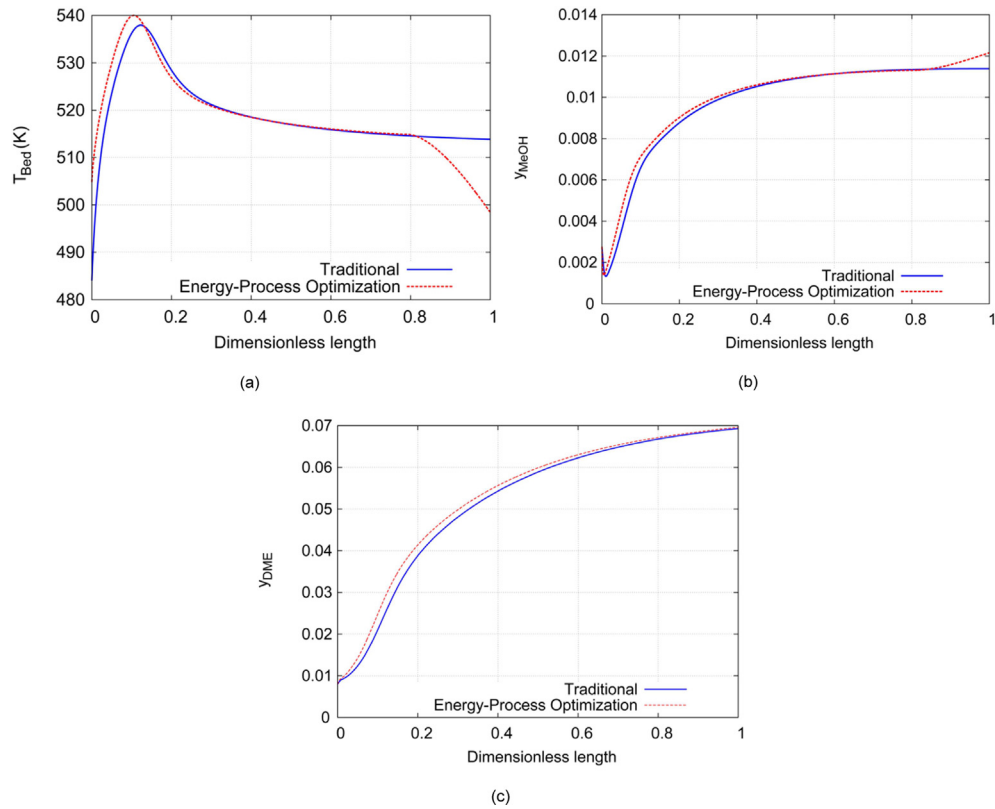


**Fig. 7.** Profile comparison between the traditional; the process optimization; and the energy process optimization for (a) temperature; (b) methanol mole fraction and (c) dimethyl ether mole fraction in dimethyl ether synthesis process.

**Table 3**

Comparison of the traditional process; the process optimization and the energy process optimization.

|                        |      | Traditional | Process optimization | Energy process optimization |
|------------------------|------|-------------|----------------------|-----------------------------|
| Length ratio           | —    | 0.7/0.3     | 0.547/0.463          | 0.527/0.473                 |
| Shell side temperature | K    | 524         | 520.09               | 520.02                      |
| Carbon conversion      | —    | 0.2149      | 0.2914               | 0.2977                      |
| Methanol mole fraction | —    | 0.063922    | 0.067703             | 0.06782                     |
| Energy from Steam      | GJ/y | 190,295     | 193,683              | 193,736                     |
| Total revenue          | €/y  | 45,844,440  | 47,529,778           | 47,580,869                  |

enhancing the energy production from steam generation. For such purpose a model-based integrated energy process optimization was employed, the mathematical model for the overall reactor system of the methanol synthesis, including the water-cooled reactor, the gas-cooled reactor, and the preliminary separation is developed and implemented as set of differential-algebraic constraints (leading to the boundary value problem due to the syngas preheating) in the optimization procedure. A series of sensitivity analysis showed the extent of the effect from the manipulation of

**Table 4**

Comparison of the traditional process and the energy process optimization.

|                              |      | Traditional | Energy process optimization |
|------------------------------|------|-------------|-----------------------------|
| Length ratio                 | —    | 1.0/0.0     | 0.78/0.22                   |
| Shell temperature            | K    | 513         | 513.4                       |
| Carbon conversion            | —    | 0.5038      | 0.5087                      |
| Methanol mole fraction       | —    | 0.011388    | 0.012150                    |
| Dimethyl ether mole fraction | —    | 0.069311    | 0.069612                    |
| Steam produced               | GJ/y | 207,021     | 212,312                     |
| Total revenue                | €/y  | 34,701,633  | 35,014,810                  |

the selected optimization parameters and provided a first approach to understand the importance of considering the whole reaction system into the optimization. The review of the reactor series within the framework of an energy-process optimization for a medium-size methanol plant leads to 1.7 M€/y of additional profit for the methanol synthesis process, all of this without a substantial modification of the process scheme that would involve a great amount of capital investment, while the inclusion of the dimethyl ether synthesis reaction as a further stage in the process increases the carbon conversion from 30% in the methanol process to about 50% in the methanol/dimethyl ether synthesis process, this implies a series of technical and economic advantages such as the reduction of compression costs in the recycle operation reflected in a more efficient use of raw materials. This study is in line with the current trend of investigations that look for process economization through the detailed modeling, simulation and optimization.

## Appendix A. Reaction kinetics

The kinetic parameters for the three reaction involved in methanol synthesis reaction are listed in Table A.1, while the adsorption equilibrium constants and reaction equilibrium constants are summarized in Table A.2 and Table A.3 respectively.

**Table A.1**

Kinetic parameters for the methanol synthesis reaction.

| $k^a$ | $A$                    | $B$      |
|-------|------------------------|----------|
| $k_1$ | $4.89 \times 10^7$     | -113,000 |
| $k_2$ | $9.641 \times 10^{11}$ | -152,900 |
| $k_3$ | $1.09 \times 10^5$     | -87,500  |

$$^a k = A \exp(B/R T)$$



**Table A.2**  
Adsorption equilibrium constants for the methanol synthesis reaction.

| $K^a$                    | A                     | B      |
|--------------------------|-----------------------|--------|
| $K_{CO}$                 | $2.16 \times 10^{-5}$ | 98,388 |
| $K_{CO_2}$               | $7.05 \times 10^{-7}$ | 61,700 |
| $K_{H_2O}/K_{H_2}^{0.5}$ | $6.37 \times 10^{-9}$ | 84,000 |

$$^a K = A \exp(B/R \cdot T)$$

**Table A.3**  
Reaction equilibrium constants for the methanol synthesis reaction.

| $K_p^a$  | A                       | B       |
|----------|-------------------------|---------|
| $K_{p1}$ | $2.391 \times 10^{-13}$ | 98,388  |
| $K_{p2}$ | $1.068 \times 10^2$     | -39,683 |
| $K_{p3}$ | $2.554 \times 10^{-11}$ | 58,705  |

$$^a K_p = A \cdot \exp(B/R \cdot T)$$

The kinetic parameters and the adsorption equilibrium constants for the dimethyl synthesis reaction are listed in Table A.4 while the reaction equilibrium constant is given by (A.1).

**Table A.4**  
Kinetic parameters and adsorption equilibrium constants for the dimethyl ether synthesis reaction.

| $k^a$        | A                      | B        |
|--------------|------------------------|----------|
| $k_4$        | $1.028 \times 10^{10}$ | -105,000 |
| $K_{CH_3OH}$ | $7.9 \times 10^{-7}$   | 70,500   |
| $K_{H_2O}$   | $8.47 \times 10^{-5}$  | 41,100   |

$$^a k = A \cdot \exp(B/R \cdot T)$$

$$K_{C4} = \frac{2835.2}{T} + 1.675 \cdot \ln T - 2.39 \times 10^{-4} - 0.21 \times 10^{-6} \cdot T^2 - 13.36 \quad (A.1)$$

## Appendix B. Auxiliary correlation

Several correlation were used in the simulation for the estimation of the different properties of the substances employed, these are listed in Table B.1,

**Table B.1**  
Correlations employed for the estimation of properties.

| Property                                    | Correlation                            | Reference |
|---|--|-----------|
| Gas viscosity of pure substances            | –                                      | [23]      |
| Viscosity of the gas mixture                | Wilke                                  | [29]      |
| Gas thermal conductivity of pure substances | –                                      | [23]      |
| Thermal conductivity of the gas mixture     | Mason and Saxena                       | [29]      |
| Binary diffusivity of pure substances       | Fuller, Schettler and Giddings         | [29]      |
| Diffusivity in multicomponent gas mixture   | Wilke                                  | [23]      |
| Bulk diffusion in pores                     | $D_e^j = D_{im} \frac{\epsilon}{\tau}$ | [23]      |

### Heat transfer correlations

The overall heat transfer coefficient between the bulk gas in the tube side and the boiling water in the WaC reactor or the fresh inlet syngas in the GaC reactor in the shell side is given by the correlation in Eq. (B.1)

$$U = \left[ \frac{1}{h_i} + \frac{A_i \ln\left(\frac{D_o}{D_i}\right)}{2\pi L k} + \frac{A_i}{A_o h_o} \right] \quad (B.1)$$

Where the convective heat transfer coefficient of the bulk phase  $h_i$  flowing in the tube side is obtained from a Chilton Colburn analogy [30]:

$$\frac{h_i}{c_{p,mix} G} \left( \frac{c_{p,mix} \mu_{mix}}{k_f} \right)^{\frac{2}{3}} = \frac{0.458}{\epsilon_B} \left( \frac{d_p G}{\mu_{mix}} \right)^{-0.407} \quad (B.2)$$

The convective heat transfer coefficient for the shell side depend of the type of the reactor, as a result, for the boiling water in the WaC reactor the Motinski correlation was employed [23]:

$$h_o = 3.75 \times 10^{-5} P_c^{0.69} \left( \frac{q}{A} \right)^{0.7} \left[ 1.8 \left( \frac{P}{P_c} \right)^{0.17} + 4 \left( \frac{P}{P_c} \right)^{1.2} + 10 \left( \frac{P}{P_c} \right)^{10} \right] \quad (B.3)$$

The maximum heat flux  $q/A$  is calculated from the Cichelli–Bonilla correlation [23]:

$$\left( \frac{q}{A} \right)_{\max} = 0.368 \left( \frac{P}{P_c} \right)^{0.35} \left( 1 - \frac{P}{P_c} \right)^{0.9} \quad (B.4)$$

The convective heat transfer coefficient for the fresh inlet gas flowing in the shell side of the GaC reactor is obtained from the Churchill and Bernstein correlation [23]:

$$\overline{Nu}_D = 0.3 + \frac{0.62 Re_D^{1/2} Pr^{1/3}}{\left[ 1 + (0.4/Pr)^{2/3} \right]^{1/4}} \left[ 1 + \left( \frac{Re_D}{282000} \right)^{5/8} \right]^{4/5} \quad (B.5)$$

## Nomenclature

|             |  |
|-------------|--|
| $A_i$       | internal area of the tube [m <sup>2</sup> ]  |
| $C_i$       | molar concentration for component i [mol/m <sup>3</sup> ]  |
| $c_{p,mix}$ | specific heat of gas at constant pressure [J/kg K]   |
| $D_e^j$     | effective diffusivity of component j [m <sup>2</sup> /s]   |
| $D_i$       | internal diameter of the tube [m]  |
| $D_o$       | external diameter of the tube [m]  |
| $D_{im}$    | diffusivity for component i in a multicomponent mixture [m <sup>2</sup> /s]                                |
| $d_p$       | catalyst particle diameter [m]   |
| $F$         | molar flowrate entering the flash separator [mol/s]  |
| $f_i$       | partial fugacity of component i [bar]  |
| $G$         | cross sectional mass velocity [kg/s m <sup>2</sup> ]   |
| $K_i$       | adsorption equilibrium constant for component i in methanol synthesis reaction [bar <sup>-1</sup> ]        |
| $K_j$       | adsorption equilibrium constant for component j in dimethyl ether synthesis reaction [m <sup>3</sup> /mol] |
| $K_C$       | reaction equilibrium constant for dimethyl ether synthesis [–]   |
| $K_C$       | reaction equilibrium constant for dimethyl ether synthesis [–]   |
| $K_{EoS,i}$ | K-values from the equation of state for component i [–]  |
| $k_i$       | reaction rate constant for the reaction i [mol/kg <sub>cat</sub> s]  |
| $k_i^{eq}$  | pseudo-equilibrium constants for component i [–]   |
| $k_j'$      | pseudo-first-order rate constant for component j [mol/s m <sup>3</sup> bar]                                |

|                    |  |
|--------------------|--|
| $L$                | liquid molar flowrate leaving the flash separator [mol/s]                          |
| $M$                | mass flowrate per tube [kg/s]  |
| $MW_i$             | molar weight for component $i$ [kg/kmol]   |
| $Nu$               | Nusselt number [–]   |
| $P$                | pressure [Pa]  |
| $P_c$              | critic pressure [Pa]   |
| $Pr$               | Prandtl number [–]   |
| $r_j$              | rate of the $j$ reaction [mol/kg <sub>cat</sub> s]                                 |
| $r'_i$             | reaction rate based on volume of catalyst for component $i$ [mol/m <sup>3</sup> s] |
| $r_p$              | catalyst particle radius [m]   |
| $R$                | universal gas constant [J/mol K]   |
| $Re$               | Reynolds number [–]  |
| $T$                | temperature of the gas phase [K]   |
| $T_{shell}$        | temperature of the shell side [K]  |
| $u$                | linear velocity of gas phase [m/s]   |
| $U_{tube}$         | overall heat transfer coefficient in the tube side [W/m <sup>2</sup> K]            |
| $U_{shell}$        | overall heat transfer coefficient in the shell side [W/m <sup>2</sup> K]           |
| $V$                | vapor molar flowrate leaving the flash separator [mol/s]                           |
| $x_i$              | molar fraction of component $i$ in the liquid phase of the flash separator [–]     |
| $y_i$              | molar fraction of component $i$ in the vapor phase of the flash separator [–]      |
| $z$                | axial coordinate [m]   |
| $Z_{f,i}$          | molar fraction of component $i$ entering the flash separator [–]                   |
| $\Delta H_j^{rxn}$ | enthalpy of reaction $j$ [J/mol]   |

#### Greek letters

|               |  |
|---------------|--|
| $\epsilon_b$  | void fraction of catalytic bed [–]   |
| $\epsilon_c$  | porosity of the catalyst pellet [–]  |
| $\eta_j$      | efficiency of the $j$ reaction [–]   |
| $\mu_{mix}$   | viscosity of the mixture [Pa s]  |
| $\nu_{ij}$    | reaction coefficient of the component $i$ in reaction $j$ [–]                        |
| $\rho_{cat}$  | catalyst particle density [kg/m <sup>3</sup> ]                                       |
| $\rho_{gas}$  | density of the gas phase [kg/m <sup>3</sup> ]  |
| $\tau$        | tortuosity of the catalyst pellet [–]  |
| $\varphi_i$   | Thiele modulus of reaction $i$ [–]   |
| $\varphi_i^L$ | fugacity coefficient of component $i$ in the liquid phase of the flash separator [–] |
| $\varphi_i^V$ | fugacity coefficient of component $i$ in the vapor phase of the flash separator [–]  |
| $\omega_i$    | Mass fraction of component $i$ in the gas phase [–]                                  |

#### References

- [1] M. Hillestad, Systematic staging in chemical reactor design, *Chem. Eng. Sci.* 65 (2010) 3301.
- [2] J.-P. Lange, Methanol synthesis: a short review of technology improvements, *Catal. Today* 64 (2001) 3.
- [3] Air Liquide, Lurgi MegaMethanol, <http://www.engineering-solutions.airliquide.com/> (accessed February, 2014).
- [4] Haldor Topsøe, Topsøe Methanol, <http://www.topsoe.com/> (accessed February, 2014).
- [5] Johnson Matthey Davy Technologies, Davy Process Methanol Technology, <http://www.davyprotech.com/> (accessed February, 2014).
- [6] G. Olah, A. Goepfert, G.K. Surya Prakash, *Beyond Oil and Gas: The Methanol Economy*, Wiley, Weinheim, Germany, 2006.
- [7] M. Shahrokhi, G.R. Baghmisheh, Modeling, simulation and control of a methanol synthesis fixed-bed reactor, *Chem. Eng. Sci.* 60 (2005) 4275.
- [8] L. Chen, Q. Jiang, Z. Song, D. Posarac, Optimization of methanol yield from a lurgi reactor, *Chem. Eng. Technol.* 34 (2011) 817.
- [9] F. Manenti, S. Cieri, M. Restelli, Considerations on the steady-state modeling of methanol synthesis fixed-bed reactor, *Chem. Eng. Sci.* 66 (2011) 152.
- [10] F. Manenti, S. Cieri, M. Restelli, G. Bozzano, Dynamic modelling of the methanol synthesis fixed-bed reactor, *Comput. Chem. Eng.* 48 (2013) 325–334.
- [11] F. Manenti, S. Cieri, M. Restelli, N.M. Nascimento Lima, L.Z. Linan, G. Bozzano, Online feasibility and effectiveness of a spatio-temporal nonlinear model predictive control, in: *The Case of Methanol Synthesis Reactor*, 22 Eur. Symposium Comput. Aided Process Engineering, vol. 30, 2012, p. 867.
- [12] Z. Ravaghi-Ardebili, F. Manenti, N.M.N. Lima, L.Z. Linan, S. Cieri, M. Restelli, G. Bozzano, Preserving safety and improving yield performances in methanol processes, *Chem. Eng. Trans.* 26 (2012) 69–74.
- [13] L. Čuček, H.L. Lam, J.J. Klemes, P.S. Varbanov, Z. Kravanja, Synthesis of regional networks for the supply of energy and bioproducts, *Clean. Technol. Environ. Policy* 12 (2010) 635.
- [14] J.J. Klemes, P.S. Varbanov, S. Pierucci, D. Huisingh, Minimising emissions and energy wastage by improved industrial processes and integration of renewable energy, *J. Clean. Prod.* 18 (2010) 843.
- [15] M.R. Rahimpour, A two-stage catalyst bed concept for conversion of carbon dioxide into methanol, *Fuel Process. Technol.* 89 (2008) 556.
- [16] A. Riaz, G. Zahedi, J.J. Klemes, A review of cleaner production methods for the manufacture of methanol, *J. Clean. Prod.* 57 (2013) 19–37.
- [17] J. Ahrenfeldt, T.P. Thomsen, U. Henriksen, L.R. Clausen, Biomass gasification cogeneration – a review of state of the art technology and near future perspectives, *Appl. Therm. Eng.* 50 (2013) 1407–1417.
- [18] F. Manenti, S. Cieri, M. Restelli, N.M.N. Lima, Z.L. Lamia, Dynamic simulation of the lurgi-type reactor for methanol synthesis, *Chem. Eng. Trans.* 24 (2011) 379.
- [19] Y. Hu, Z. Nie, D. Fang, Simulation and model design of pipe-shell reactor for the direct synthesis of dimethyl ether from syngas, *J. Nat. Gas. Chem.* 17 (2008) 195–200.
- [20] B.J. Lommerts, G.H. Graaf, A. Beenackers, Mathematical modeling of internal mass transport limitations in methanol synthesis, *Chem. Eng. Sci.* 55 (2000) 5589.
- [21] G.H. Graaf, E.J. Stadhuis, A.A.C.M. Beenackers, Kinetics of low-pressure methanol synthesis, *Chem. Eng. Sci.* 43 (1988) 3185.
- [22] G. Berčić, J. Levec, Intrinsic and global reaction rate of methanol dehydration over gamma-alumina pellets, *Ind. Eng. Chem. Res.* 31 (1992) 1035.
- [23] D.W. Green, R.H. Perry, *Perry's Chemical Engineers' Handbook*, McGraw-Hill Professional Publishing, New York, NY, 2007.
- [24] R. Vakili, E. Pourazadi, P. Setoodeh, R. Eslamloueyan, M.R. Rahimpour, Direct dimethyl ether (DME) synthesis through a thermally coupled heat exchanger reactor, *Appl. Energy* 88 (2011) 1211–1223.
- [25] F. Askari, M. Rahimpour, A. Jahanmiri, A. Mostafazadeh, A. Khosravanipour Mostafazadeh, Dynamic simulation and optimization of a dual-type methanol reactor using genetic algorithms, *Chem. Eng. Technol.* 31 (2008) 513.
- [26] F. Manenti, A.R. Leon Garzon, G. Bozzano, Energy-process integration of the gas-cooled/water-cooled fixed-bed reactor network for methanol synthesis, *Chem. Eng. Trans.* 35 (2013) 1243.
- [27] Methanex Corporation, Methanex Regional Posted Contract Prices, <http://www.methanex.com> (accessed March, 2013).
- [28] R. Fornell, T. Berntsson, A. Asblad, Techno-economic analysis of a kraft pulp-mill-based biorefinery producing both ethanol and dimethyl ether, *Energy* 50 (2013) 83.
- [29] B.E. Poling, J.M. Prausnitz, J.P. O'Connell, *The Properties of Gases and Liquids*, Fifth ed., McGraw-Hill Professional Publishing, New York, NY, 2001.
- [30] J.M. Smith, *Chemical Engineering Kinetics*, Third ed., McGraw-Hill, New York, NY, 1983.